Phytochemistry 71 (2010) 726–735

Contents lists available at ScienceDirect

Phytochemistry

journal homepage: www.elsevier.com/locate/phytochem

Co-pigmentation and flavonoid glycosyltransferases in blue *Veronica persica* flowers ☆

Eiichiro Ono [a], Miho Ruike [b], Takashi Iwashita [c], Kyosuke Nomoto [b,1], Yuko Fukui [a,*]

[a] Institute for Health Care Science, Suntory Ltd., 1-1-1 Wakayamadai, Shimamoto, Mishima, Osaka 618-8503, Japan
[b] Faculty of Life Science, Toyo University, 1-1-1 Izumino, Itakura, Ora, Gunma 374-0113, Japan
[c] Suntory, Institute for Bioorganic Research, 1-1-1 Wakayamadai, Shimamoto, Mishima, Osaka 618-8503, Japan

ARTICLE INFO

Article history:
Received 30 April 2009
Received in revised form 17 December 2009
Available online 10 March 2010

Keywords:
Veronica persica
Lamiales
Flavonoid
Co-pigment
Glycosyltransferase
Glucuronosylation
Glucosylation
UGT

ABSTRACT

Glycosylation is one of the key modification steps for plants to produce a broad spectrum of flavonoids with various structures and colors. A survey of flavonoids in the blue flowers of *Veronica persica* Poiret (Lamiales, Scrophulariaceae), which is native of Eurasia and now widespread worldwide, led to the identification of highly glycosylated flavonoids, namely delphinidin 3-*O*-(2-*O*-(6-*O*-*p*-coumaroyl-glucosyl)-6-*O*-*p*-coumaroyl-glucoside)-5-*O*-glucoside (1) and apigenin 7-*O*-(2-*O*-glucuronosyl)-glucuronide (2), as two of its main flavonoids. Interestingly, the latter flavone glucuronide (2) caused a bathochromic shift on the anthocyanin (1) toward a blue hue in a dose-dependent manner, showing an intermolecular co-pigment effect. In order to understand the molecular basis for the biosynthesis of this glucuronide, we isolated a cDNA encoding a UDP-dependent glycosyltransferase (UGT88D8), based on the structural similarity to flavonoid 7-*O*-glucuronosyltransferases (F7GAT) from Lamiales plants. Enzyme assays showed that the recombinant UGT88D8 protein catalyzes the 7-*O*-glucuronosylation of apigenin and its related flavonoids with preference to UDP–glucuronic acid as a sugar donor. Furthermore, we identified and functionally characterized a cDNA encoding another UGT, UGT94F1, as the anthocyanin 3-*O*-glucoside-2″-*O*-glucosyltransferase (A3Glc2″GlcT), according to the structural similarity to sugar–sugar glycosyltransferases classified to the cluster IV of flavonoid UGTs. Preferential expression of *UGT88D8* and *UGT94F1* genes in the petals supports the idea that these UGTs play an important role in the biosynthesis of key flavonoids responsible for the development of the blue color of *V. persica* flowers.

1. Introduction

Blue flowers are rare in nature. Limited examples includes dayflower (*Commelina communis*) and cornflower (*Centaurea cyanus*), both of which produce natural supramolecules known as metalloanthocyanins in their petals (Kondo et al., 1992; Shiono et al., 2005). Those metalloanthocyanins are formed through stoichiometric self-association of metal-pigment complexes, and metal complexation of flavonoid glycosides and intermolecular hydrophobic association confer pure blue coloration on flowers (Goto and Kondo, 1991; Yoshida et al., 2009). Recent studies on the metalloanthocyanins from two *Salvia* species with blue petals showed that the pigment complex consists of six molecules each of diglycosyl anthocyanins and diglycosyl flavones, although the composition of the flavonoids within the complex is different between the two species (Kondo et al., 2001; Mori et al., 2008). In the case of the Himalayan blue poppy (*Meconopsis grandis*) has a diglucosyl flavonol as a component of the metal complex-pigment in the sky-blue flower (Yoshida et al., 2006).

Co-pigmentation, in addition to the metal complex-pigment, is also well known to cause bathochromic shift by an intermolecular association that colored anthocyanin pigments and colorless/transparent co-pigments, such as flavone glycosides stack hydrophobically in an aqueous solution (Goto and Kondo, 1991). Co-pigmentation occurs only in solution in a non-stoichiometrical way, and confers a bluish color on flowers and fruits of plants, and also during fermentation processes of wines (Boulton, 2001). Flavones/flavonols *per se* exhibit pale yellow color; however, their role as co-pigments and UV-absorbents seem to be more significant on flower coloration, serving as key modulators of anthocyanin pigments for pollinator attraction (Asen et al., 1972;

Abbreviations: MeCN, acetonitrile; UDP, uridine diphosphate; GlcA, glucuronic acid; Glc, glucose; $^{1}H\{^{13}C\}$-HMBC, heteronuclear multiple bond correlation.

☆ The DDBJ Accession Numbers for UGT88D8, UGT94C2, and UGT94F1 are AB465708, AB514128, and AB514127, respectively.

* Corresponding author. Tel.: +81 75 962 6207; fax: +81 75 962 1690.
E-mail address: Yuko_Fukui@suntory.co.jp (Y. Fukui).

[1] Present address: Nara Prefectural Small and Medium-sized Enterprises Support Corporation, Nara Prefectural Agricultural Experiment Station, 88 Shijo, Kashihara, Nara 634-0813, Japan.

0031-9422/$ - see front matter © 2010 Elsevier Ltd. All rights reserved.
doi:10.1016/j.phytochem.2010.02.008

Thompson and Meinwald, 1972). For instance, the *C*-glucosyl flavone isovitexin in the petals of the garden iris (*Iris ensata* Thunb.) is known to be a strong co-pigment co-existing with the iris anthocyanin, delphinidin 3-*O*-*p*-coumaroyl-rutinoside-5-*O*-glucoside (Yabuya et al., 1997). Moreover, apigenin 7-*O*-glucuronide and luteolin 7-*O*-glycoside have been reported as a strong co-pigment in snapdragon (*Antirrhium majus*) and wishbone flowers (*Torenia hybrida*), respectively (Asen et al., 1972; Aida et al., 2000). It is noteworthy that co-pigmentation efficiency depends on the structural affinity of modified pigments to co-pigments, as well as their concentrations, and vacuolar pH of the solution (Fukui et al., 2003). The fact that flavonoid composition in flowers with similar color varies among different species highlights the importance of the structural diversity of this class of pigments for developing ornamentals with novel flower colors (Katsumoto et al., 2007).

Plant secondary metabolites, or specialized metabolites, have extraordinary diverse core structures that are often further elaborated through modifications including glycosylation (Harborne and Baxter, 1999). Specific plant lineage has specialized flavonoids with unique glycosylation pattern, that are a consequence of the general differentiation of regio-specificity of the UGT enzyme followed by local differentiation of sugar donor specificity in a lineage-specific manner (Vogt and Jones, 2000; Noguchi et al., 2008, 2009). For example, flavone 7-*O*-glucuronide, a specialized metabolite of Lamiales plants, is produced by a flavonoid 7-*O*-glucuronosyltransferase (F7GAT), which is considered to be locally differentiated from flavonoid 7-*O*-glucosyltransferase (F7GlcT) by acquiring the binding specificity to UDP–glucuronic acid (UDP–GlcA) instead of UDP–glucose (Harborne, 1963; Yoshida et al., 1993; Hirotani et al., 1998; Yamazaki et al., 2003; Noguchi et al., 2009).

Here, we describe identification and functional characterization of two novel UGTs responsible for the blue flower color of *Veronica persica* Poiret (Lamiales, Scrophulariaceae), which is native to Mediterranean area and domesticates throughout temperate zone (Fig. 1A). Most recently, flavonoids that accumulated in the flowers of this plant were also reported (Mori et al., 2009) after this submission was received. Here we show the cloning of the two *V. persica* UGTs, one is involved in the biosynthesis of anthocyanin glycosides, and the other in the biosynthesis of flavone glucuronide co-pigments. Observation of bathochromic shift of the anthocyanin **1** by the addition of flavone glucuronide **2** *in vitro* further underscores the significance of the glycosylation of these major flavonoids for color development of the blue petals of *V. persica*.

2. Results and discussion

2.1. Measurement of pH and the $L^*a^*b^*$ color of Veronica petals

Vacuolar pH significantly affects the coloration of anthocyanin pigments and varies in each species. As the vacuole is the largest organella in petal cells, the value of pressed petal juice is often measured as the approximate vacuolar pH (Fukada-Tanaka et al., 2000; Verweij et al., 2008). The pH value of the petal juice of *V. persica* was estimated to be 6.2, which is relatively high compared to that of carnation and rose petals (Fukui et al., 2003; Katsumoto et al., 2007). The intact petal showed characteristic spectra with the two λ_{max} peaks at 580.4 and 628.8 nm (Fig. 1B). The petal surface colors in an $L^*a^*b^*$ colorimetric value were L^*; 48.01, a^*; 17.67, b^*; −33.49 and the hue was 297.8° (Fig. 1C).

2.2. Identification of flavonoid glycosides

High-resolution time-of-flight MS (HR-TOF-MS) analysis of isolated compounds **1** and **2** gave molecular ions at *m*/*z* 1081.2876, $[M]^+$ (calcd. 1081.2825, err: +4.7 ppm) and 623.1251, $[M+H]^+$ (calcd. 623.1248, err: +0.5 ppm), respectively. These values correlated to the masses calculated using their molecular formulae: $C_{51}H_{53}O_{26}$ and $C_{27}H_{26}O_{17}$, respectively. The λ_{max} of **1** was 541 nm in 10% MeCN in H_2O with 0.1% TFA.

After acid hydrolysis, the HPLC analysis of **1** indicated the presence of delphinidin (ret. time: 4.0 min, λ_{max}: 538 nm). We were able to establish full assignment data for the ^1H NMR and ^{13}C NMR spectra for **1** and **2** (see Supplementary Tables 1 and 2, respectively), using $^1H\{^{13}C\}$-HSQC, $^1H\{^{13}C\}$-HMBC, TOCSY, DQF-COSY, and ROESY. The ^1H NMR and ^{13}C NMR spectroscopic data of **1** indicated the presence of three glucosyl residues and two *p*-coumaroyl moieties. In the case of compound **1**, the analysis of the $^1H\{^{13}C\}$-HMBC established that the hydroxyl groups at the

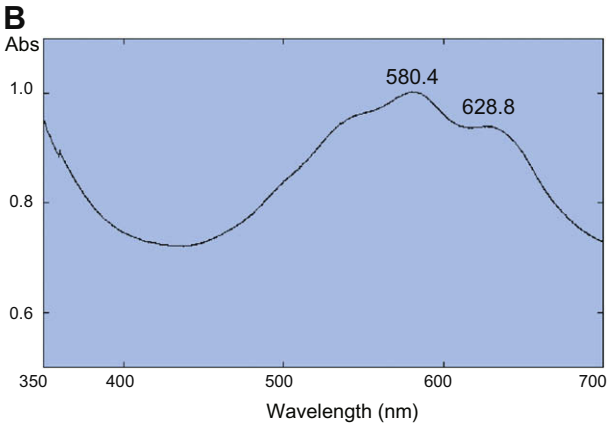

C

molar ratio	L *	a *	b *	H K	max (nm)	OD
Petal	48.01	17.67	-33.49	297.8	580, 629	
in vitro						
1 : 0	43.52	42.28	-56.75	306.6	615	1
1 : 1	41.94	38.64	-59.36	303.0	614	1.021
1 : 2	40.65	36.79	-60.30	301.4	632	1.031
1 : 3	39.96	34.98	-60.34	300.1	630	1.038
1 : 4	39.46	33.41	-60.02	299.1	639	1.045
1 : 5	39.59	31.65	-59.18	298.1	641	1.035
1 : 6	39.84	29.92	-58.13	297.2	645	1.037

Fig. 1. *Veronica persica* flowers and co-pigment effect. (A) Bluish flowers of *Veronica persica* (B) absorption spectra of intact petals of *V. persica* (C) $L^*a^*b^*$ color value and visible spectral data of co-pigment assay. Co-pigment analyses of compound **1** with **2** were measured in a McIlvaine buffer (pH 6.2). Compound **1** was dissolved in 1 mM concentration, and **2** was added in 1–6 equivalent to **1**. The hue (H) was shifted to blue in molar ratio dependent. The molar ratio is anthocyanin **1**: flavone **2**.

C-3 in the C-ring and C-5 positions in the A-ring of the delphinidin nucleus were bound with Glc-1 and Glc-2, respectively. In addition, the resonances of methylene protons at the H-6 position in Glc-1 (δ 4.38) correlated with the carbonyl carbon in the *p*-coumarate-1 (δ 168.8), and those of methylene protons at the H-6 position in Glc-3 (δ 4.17) correlated with the carbonyl carbon in the *p*-coumarate-2 (δ 168.5), those of the anomeric proton in Glc-3 (δ 4.75) correlated with the ^{13}C signal of the C-2 carbon in the Glc-1 (δ 84.5), and this carbon signal shifted to a lower magnetic field. Therefore, **1** was deduced to be delphinidin 3-*O*-(2-*O*-(6-*O*-*p*-coumaroyl-glucosyl)-6-*O*-*p*-coumaroyl-glucoside)-5-*O*-glucoside (Fig. 2).

Anthocyanin **1** is identical to one of the compounds mentioned in the recent study on flavonoids in *V. persica* flowers (Mori et al., 2009) being submitted after our own paper. The malonylated form of anthocyanin **1** has also been reported in *Ajuga reptans* (Lamiales, Lamiaceae) and *V. persica* (Terahara et al., 1996; Yoshida et al., 2009). Analysis using high-resolution LC-TOF-MS established that both anthocyanin **1** and its mono-malonylated form accumulate as main pigments in the blue petals in the ratio 4:6 in the fresh petals.

On the other hand, **2** had an apigenin nucleus and two glucuronosyl moieties in the molecule. In the $^{1}H\{^{13}C\}$-HMBC analysis of **2**, cross-peaks between H-1 of GlcA-2 (δ 4.68) and C-2 of GlcA-1 (δ 83.9) were observed, and a ROE was observed between the H-1 of GlcA-1 (δ 5.40) and both H-6 and H-8 protons in the A ring of the apigenin nucleus (δ 6.45 and 6.76). Therefore, **2** was deduced to be apigenin 7-*O*-(2-*O*-β-glucuronosyl)-β-glucuronide (Fig. 2). The structure of **2** was identical to a flavone glucuronide previously isolated from *Perilla ocimoides* leaves (Lamiales, Lamiaceae), and also mentioned in the recent study on *V. persica* flowers (Yoshida et al., 1993; Mori et al., 2009).

2.3. Co-pigment assay

Importance of flavone glycosides as co-pigments has been documented in several species (Asen et al., 1972; Yabuya et al., 1997; Fukui et al., 2003). To investigate whether that is the case with the flavone **2** on anthocyanin **1**, the bathochromic shift of **2** on **1** was measured in McIlvaine buffer (pH 6.2) (Fig. 1C). When **2** was added to **1** in various molar ratio, a remarkable bathochromic shift of the absorbance maximum ($\Delta\lambda_{max}$) was observed in a dose-dependent manner; the original λ_{max} of **1**, which is 615 nm, was shifted toward longer wavelength as the molar ratio of **2**–**1** increases. Under our experimental conditions, the addition of six equivalents of **2**–**1** resulted in the maximum bathochromic shift to 645 nm. Moreover, the hue of this solution was 297.2° in the $L^*a^*b^*$ colorimetric value, which is in the range of that of an intact petal (297.8°). These results indicate that **2** has a strong co-pigment effect on **1** under conditions where the molar ratio of **1**–**2** is 1:6, respectively. Actually, pigments **1** and co-pigment **2** were estimated to be present in a molar ratio of 1:9 in the fresh petals, which roughly fits with the result from the *in vitro* co-pigment assay (Fig. 1C). Therefore, these data strongly suggest that this co-pigmentation occurs *in planta* and supposedly influences the blue coloration of *V. persica* flowers.

These data are remarkable since only a small bathochromic shift of λ_{max} was observed when 5 equivalents of **2** were added to malonylated **1** (Mori et al., 2009). These contrasting results suggest that the malonyl moiety on **1** sterically exerts an inhibitory effect on intermolecular stacking which, in turn, reduces the co-pigmentation effect. This is then consistent with the previous notion that structural affinity between anthocyanin pigment and flavone co-pigment is critical for intermolecular stacking (Fukui et al., 2003). The data also implicate that, among various flavonoids existing in bluish flowers, only selected combinations of anthocyanins and flavones with specific and proper modifications display a co-pigmentation effect.

Considering the color alteration of anthocyanins upon pH changes, we therefore conclude that the underlying reason for the bluish hue of the *V. persica* flowers is provided by (1) the accumulation of highly aromatic acylated delphinidin-type anthocyanins, (2) co-pigmentation by the proper combination of anthocyanin pigment **1** and flavone co-pigment **2**, and (3) the relatively high vacuolar pH in the petals (estimated to be 6.2).

2.4. Molecular cloning of UGT88D8

The significant bathochromic effect of co-pigment **2** on anthocyanin pigment **1** prompted us to investigate genes responsible for biosyntheses of those flavonoids. Flavone 7-*O*-glucuronide is known to be a specialized metabolite of Lamiales plants; therefore, it is expected that a flavonoid 7-*O*-glucuronosyltransferase (F7GAT) is also present in *V. persica* (Noguchi et al., 2009). To investigate whether 7-*O*-glucuronosylation activity on apigenin exists in *V. persica*, we first conducted enzyme assays using crude extracts prepared from *V. persica* petals. The results show that the extracts contain a significant level of 7-*O*-glucuronosylation activity on

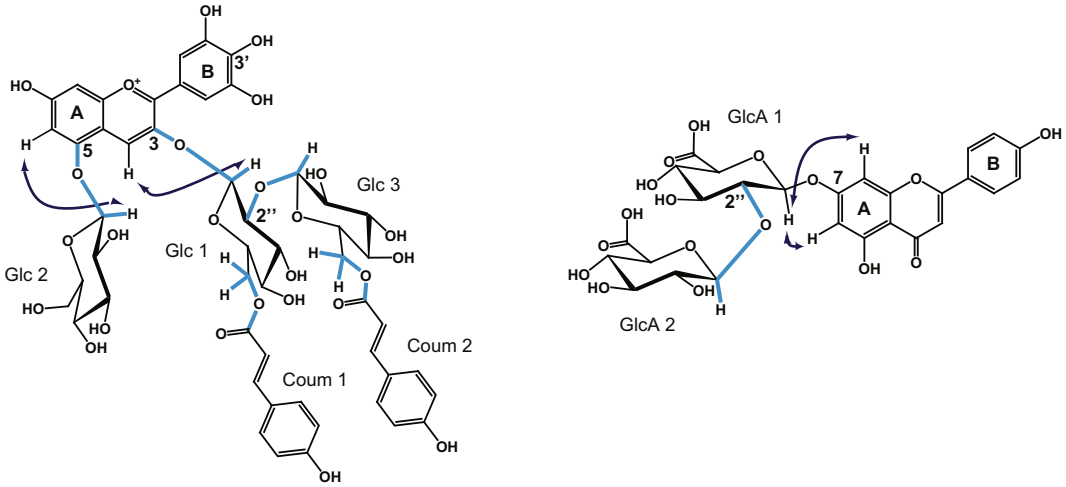

1. Delphinidin 3-*O*-(2-*O*-(6-*O*-*p*-coumaroyl-glucosyl)-6-*O*-*p*-coumaroyl-glucoside)-5-O-glucoside **2.** Apigenin 7-*O*-(2-*O*-glucuronosyl)-glucuronide

Fig. 2. Flavonoid structures of *Veronica persica*. Major anthocyanin pigment **1** and flavone co-pigment **2** isolated from the blue petals. Solid lines indicate $^{1}H\{^{13}C\}$-HMBC. Arrows indicate ROE. (For interpretation of the references to color in this figure legend, the reader is referred to the web version of this article.)

apigenin, which was dependent on UDP–glucuronic acid (UDP–GlcA) (Supplementary Fig. 1). The increased level of apigenin 7-*O*-glucuronide was accompanied with a decrease in apigenin level, thereby demonstrating that UGT enzymes should be involved in the co-pigment formation. Moreover, crude enzymes prepared from leaves also showed glucuronosylation activity on apigenin (Supplementary Fig. 1).

Detection of the glucuronosylation activity on apigenin *in planta* prompted us to clone UGT genes responsible for the enzyme activity. A cDNA fragment showing a significant sequence similarity to the snapdragon (Lamiales, Scrophulariaceae, *Antirrhinum majus*) F7GAT (UGT88D4) gene was amplified in cDNAs prepared from the petals by reverse transcription-polymerase chain reaction (RT-PCR) (Ono et al., 2006; Noguchi et al., 2009). Its full-length sequence was determined by the rapid amplification of cDNA ends (RACE) method and was designated as UGT88D8 according to the nomenclature of UGTs (Mackenzie et al., 1997). UGT88D8 (1362 bp) contains an open reading frame (ORF) corresponding to a protein of 454 amino acids in length with a predicted molecular mass of 50.1 kDa, and shows 61% amino acid sequence identity to snapdragon F7GAT; therefore, it is most likely to be a Lamiales F7GAT.

2.5. Biochemical characterization of UGT88D8

To determine the biochemical property of UGT88D8, the recombinant protein was heterologously expressed as a His(x6)-tag fused chimeric protein in *Escherichia coli* and purified with a nickel-affinity column (Fig. 3A). The purified UGT88D8 was subjected to enzymatic assays. In the reaction with apigenin and UDP–GlcA as substrates, UGT88D8 gave a product at the same retention time of the authentic apigenin 7-*O*-glucuronide when analyzed by HPLC (Fig. 3B). The product exhibited a molecular ion at *m*/*z* 445.0759 $[M-H]^-$, which was consistent with the mass calculation of apigenin 7-*O*-glucuronide ($C_{21}H_{17}O_{11}$, 445.0771, err: +3.1 ppm). Furthermore, LC–MS/MS analysis confirmed that a fragment ion of the product is consistent with apigenin (*m*/*z* 269.0450 $[M-H]^-$). No significant product peak was observed in the reaction mixture without UDP–GlcA. In sharp contrast to UDP–GlcA, neither UDP–galactose nor UDP–glucose served as an effective sugar donor for the catalysis (Fig. 3C), demonstrating that UGT88D8 catalyzes glucuronosylation of apigenin at the 7-hydroxy group.

Next, we tested various flavonoids as the possible sugar acceptors for UGT88D8. The most favorable substrate among tested for UGT88D8 *in vitro* was apigenin, followed by scutellarein and crysoeriol, all of which have an hydroxyl group at 4′-position in the B-ring of flavone backbone (Fig. 3D). This finding is in accordance with the observation that apigenin 7-*O*-(2″-*O*-glucuronosyl)-glucuronide is the most abundant flavone in the petals, suggesting that UGT88D8 plays major role in the accumulation of this flavone. The sugar acceptor preference of UGT88D8 was similar to those of non-*Scutellaria* F7GATs, perilla UGT88D7, sesame UGT88D6, and snapdragon UGT88D4, and apparently distinguishable at the enzyme activity level from *Scutellaria* F7GATs, *S. baicalensis* UGT88D1 and *S. laeteviolaceae* UGT88D5, which specifically catalyze flavones with *ortho*-substituents at the 7-position, e.g., baicalein (Hirotani et al., 2000; Noguchi et al., 2009). The optimal pH was tested in a range from 5.0 to 9.5, and estimated to be 8.0 for the catalysis of UGT88D8 on apigenin (Fig. 3E). The calculated *km* values for apigenin and UDP–GlcA were 10.72 ± 1.67 and 36.55 ± 8.66 μM, respectively. The *k*cat value for apigenin was determined to be 7.42 ± 0.36 s^{-1}. These kinetic parameters were comparable to those of a perilla F7GAT, UGT88D7 (Noguchi et al., 2009), demonstrating that UGT88D8 is an orthologous F7GAT of *V. persica*.

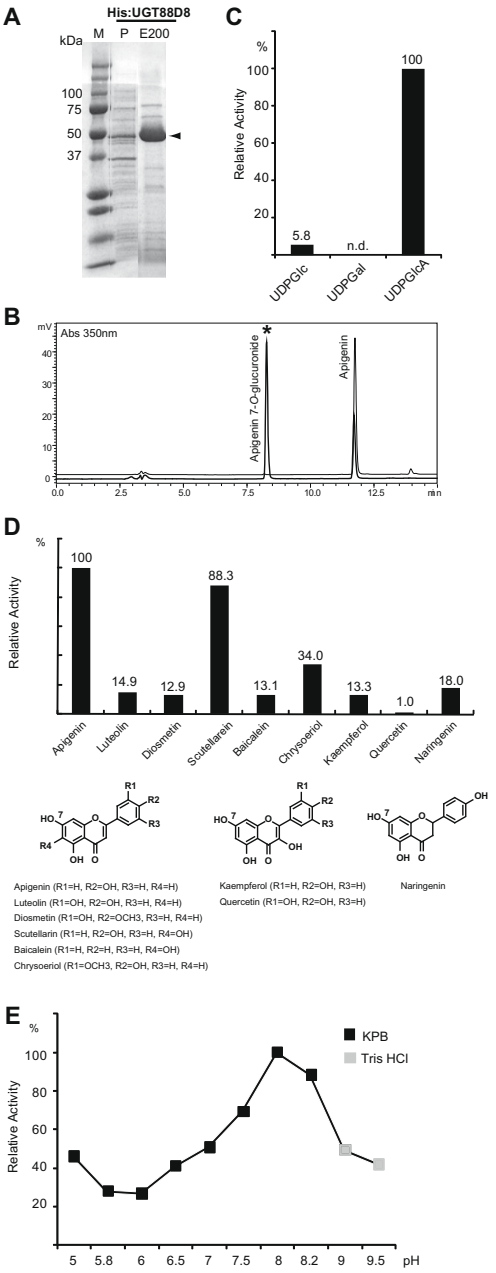

Fig. 3. Biochemical characterization of UGT88D8. (A) The recombinant His(-x6)::UGT88D8 fusion protein (arrowhead) was expressed in *E. coli*, purified by a His Trap™ HP column, and detected using Coomassie Brilliant Blue (CBB) staining. M: molecular size marker, P: pellet fraction, S: soluble fraction, F: flow throw, E50, E200, and E500: eluted fraction with 50 mM, 200 mM, and 500 mM imidazole, respectively. (B) Chromatograms at abs 350 nm of reaction mixtures of UDPGA and apigenin in the absence (thin line) or presence (thick line) of the enzyme. The asterisk indicates a new product given by UGT88D8. (C) Relative sugar donor specificity of UGT88D8. Apigenin was used as the sugar acceptor. The highest specific activity on UDP–GlcA is set as 100%. n.d. indicates "not detected". (D) Sugar acceptor specificity of UGT88D8. Relative activities toward 100 μM solutions of flavonoids are shown. The highest glucuronosylating activity toward apigenin is taken to be 100%. (E) Optimal pH of UGT88D8 for apigenin was tested in a range from pH 5 to 9.5 using potassium phosphate buffer (KPB) for pH 5 to 8.2 (black) and Tris–HCl buffer for pH 9 and 9.5 (gray). The highest activity was taken to be 100%.

2.6. Phylogenetic analysis of UGT88D8

It is generally considered that flavonoid UGTs with the same regio-specificity toward flavonoids form distinct phylogenetic clusters beyond species regardless of sugar donor specificity

(Noguchi et al., 2008). Based on this consideration, UGT88D8 was successfully identified from *V. persica*. A neighbor-joining phytogenetic tree showed that UGT88D8 lies in the functional cluster IIIb of flavonoid UGTs with the regio-specificity for 7-position of flavonoids (Ono et al., 2006; Noguchi et al., 2009) (Fig. 4A). Furthermore, UGT88D8 is a new member of the Lamiales F7GAT subcluster, and is structurally more similar to non-*Scutellaria* F7GATs such as snapdragon F7GAT (UGT88D4) than to *Scutellaria* F7GATs in this subcluster. These data support the consistency between the biochemical similarity and the taxonomic relationship among F7GATs.

Recent study shows that a conserved Arg residue in the C-terminal PSPG-box of Lamiales F7GATs is crucial for the recognition of the anionic carboxylate of the glucuronic acid moiety of UDP–GlcA (Noguchi et al., 2009). Sequence alignment analysis indicates that Arg352 of UGT88D8 corresponds to the Arg residue conserved in F7GATs (Supplementary Fig. 2), suggesting that this Arg residue contributes to the exclusive specificity of UGT88D8 for UDP–GlcA as a sugar donor (Fig. 3C). On the other hand, the amino acid residue indispensable for the sugar donor specificity of another glucuronosyltransferase, BpGAT (UGT94B1) from red daisy (*Bellis perennis*), to UDP–GA is Arg25 located at the N-terminus, as opposed to Arg352 of UGT88D8 (Fig. 4B, Supplementary Fig. 2) (Sawada et al., 2005; Osmani et al., 2008). These results suggest that the Arg residues that are important for the sugar donor specificity of F7GATs and BpGAT to UDP–GA occurred independently as a consequence of the convergent evolution (Noguchi et al., 2009). This flexibility of altering sugar donor specificity by substitution of only a few amino acids in turn might explain why UGTs with equivalent regio-specificities grouped in a clade often exhibit various substrate specificities for sugar donors.

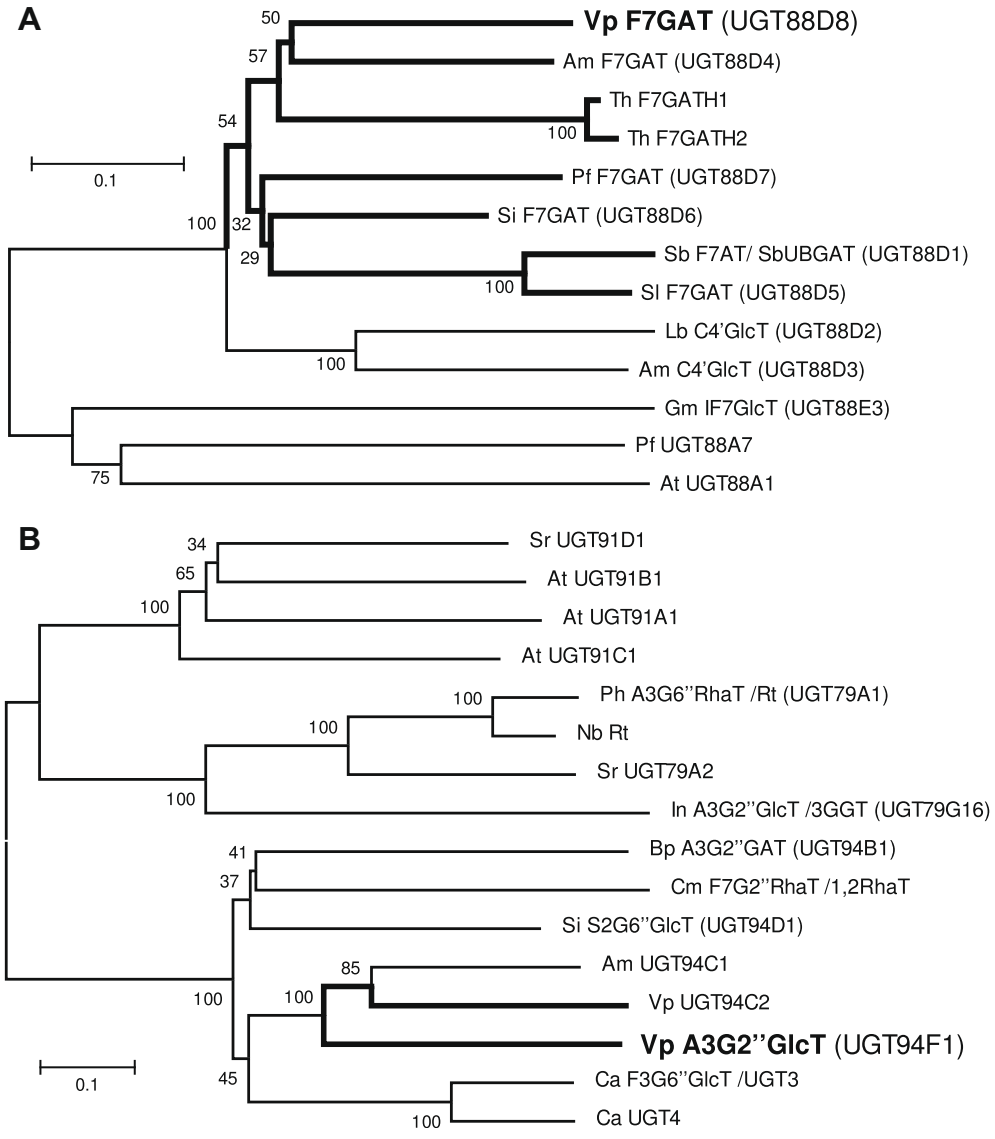

Fig. 4. Phylogenetic trees of UGT88-related UGTs (upper) and sugar–sugar UGTs (lower). Unrooted trees were constructed using MEGA ver. 4.1 software (http://www.megasoftware.net/) based on the CLUSTAL-W multiple alignment using neighbor-joining (NJ) (Thompson et al., 1994; Tamura et al., 2007). The solid lines indicate the Lamiales F7GAT cluster in the upper tree. The percentage of replicate trees in which the associated taxa clustered together in the bootstrap test (1000 replicates) is shown next to the branches. The accession numbers of these UGTs are available in previous reports (Noguchi et al., 2008, 2009; Masada et al., 2009). Vp: *Veronica persica*, Am: *Antirrhinum majus*, Th: *Torenia hybrida*, Pf: *Perilla frutescens*, Si: *Sesamum indicum*, Sb: *Scutellaria baicalensis*, Sl: *Scutellaria laeteviolacea*, Lb: *Linaria bipartite*, Gm: *Glycine max*, At: *Arabidopsis thaliana*, In: *Ipomoea nil*, Ph: *Petunia hybrida*, Sr: *Stevia rebaudiana*, Nb: *Nierembergia*, Bp: *Bellis perennis*, Cm: *Citrus maxima*, Ca: *Catharanthus roseus*.

2.7. Identification and characterization of UGT94F1

Identification of UGT88D8 led to further exploration of the second enzyme catalyzing 2″-*O*-glucuronosylation of sugar moiety of apigenin 7-*O*-glucuronide, thereby completing the structure of co-pigment **2**. Considering that the functional cluster IV of flavonoid UGTs represented by BpGAT (UGT94B1) has been known to catalyze glycosylation of sugar moiety in flavonoid glycosides (sugar–sugar glycosylation) with a regio-specificity to the 2 or 6 position of sugar moiety but not of flavonoid aglycones, the second GAT is likely to be a member of this cluster (Fig. 4B) (Frydman et al., 2004; Sawada et al., 2005; Morita et al., 2005; Noguchi et al., 2008; Masada et al., 2009). In addition to the previous observation of **2** in *Perilla* (Yoshida et al., 1993), acacetin 7-*O*-(2-*O*″-glucuronosyl)-glucuronide was reported in *Clerodendrum trichotomum* (Verbenaceae), which lies within the Lamiales order (Okigawa et al., 1971; Harborne and Baxter, 1999). Therefore, as is the case of the first GAT (F7GAT), the second GAT may also be widespread in Lamiales plants. Based on this rationale, we isolated two candidate cluster IV UGT genes (UGT94C2 and UGT94F1) from *V. persica* petals by RT-PCR (Fig. 4B). UGT94C2 (1380 bp) and UGT94F1 (1356 bp); these encode putative proteins of 460 and 452 amino acids in a length with the predicted molecular mass of 52.4 and 51.0 kDa, respectively. They showed highest structural similarity to snapdragon UGT94C1 of unknown function (Ono et al., 2006); UGT94C2 and UGT94F1 exhibit 58% and 49% identities at amino acid level to UGT94C1, respectively, and 45% sequence identity to each other.

To test biochemical activities of the two UGTs, their His-tag fused proteins were heterologously expressed in *E. coli* and then purified through a nickel-affinity column (Fig. 5A). Unexpectedly, however, both of the recombinant proteins did not show a detectable level of glucuronosylation activity for apigenin 7-*O*-glucuronide. For this reason, we further searched for flavonoids other than apigenin 7-*O*-glucuronide as possible substrates for UGT94C2 and UGT94F1. Inspired by the fact that anthocyanin **1** has a delphinidin 3-*O*-sophoroside structure (β1 → 2 di-glucoside), we then tested whether these two UGTs would glucosylate the 2″-hydroxy group of sugar moiety of delphinidin 3-*O*-glucoside. The data clearly show that UGT94F1, but not UGT94C1, accepts delphinidin 3-*O*-glucoside as a substrate. Therefore, UGT94F1 turned out to be a UDP–glucose-dependent glucosyltransferase toward delphinidin 3-*O*-glucoside (Fig. 5B). The product exhibited a molecular ion at *m*/*z* 627.1568 $[M]^+$, which was consistent with the mass calculation of delphinidin di-glucoside ($C_{27}H_{31}O_{17}$, 627.1556, err: +1.9 ppm). The $^1H\{^{13}C\}$-HMBC spectrum showed a cross-peak between the H-1 of glucose-3(Glc-3) (δ 4.71, d, J = 7.8 Hz) and the C-2 of glucose-1 (δ 83.47), consistent with covalent linkage between two glucose moieties in a β-D-glucosyl-(1 → 2)-β-D-glucoside structure (Supplementary Table 1). Thus, the product was determined to be delphinidin 3-*O*-(2-*O*-glucosyl)-glucoside (delphinidin 3-sophoroside) (Harborne and Baxter, 1999). In addition, UGT94F1 also glucosylated 3-*O*-glucosides of cyanidin and pelargonidin although both anthocyanins have not been found in *V. persica* petals. In sharp contrast, UGT94F1 did not show glucosylation activity for either flavonol 3-*O*-glucosides (kaempferol and quercetin), anthocyanidin aglycones (cyanidin and delphinidin), or their 3,5-*O*-di-glucosides. This sugar acceptor specificity was similar to that of *Ipomoea nil* dusky/3GGT/UGT79G16 enzyme (Morita et al., 2005). Given that both *V. persica* and *I. nil* accumulate anthocyanin 3,5-*O*-glucoside derivatives as their primary pigments in petals, glucosylation on the 2″-hydroxy group of sugar moiety of anthocyanidin 3-*O*-glucosides could occur prior to 5-*O*-glucosylation *in planta*. The *km* values for delphinidin 3-*O*-glucoside and UDP–glu-

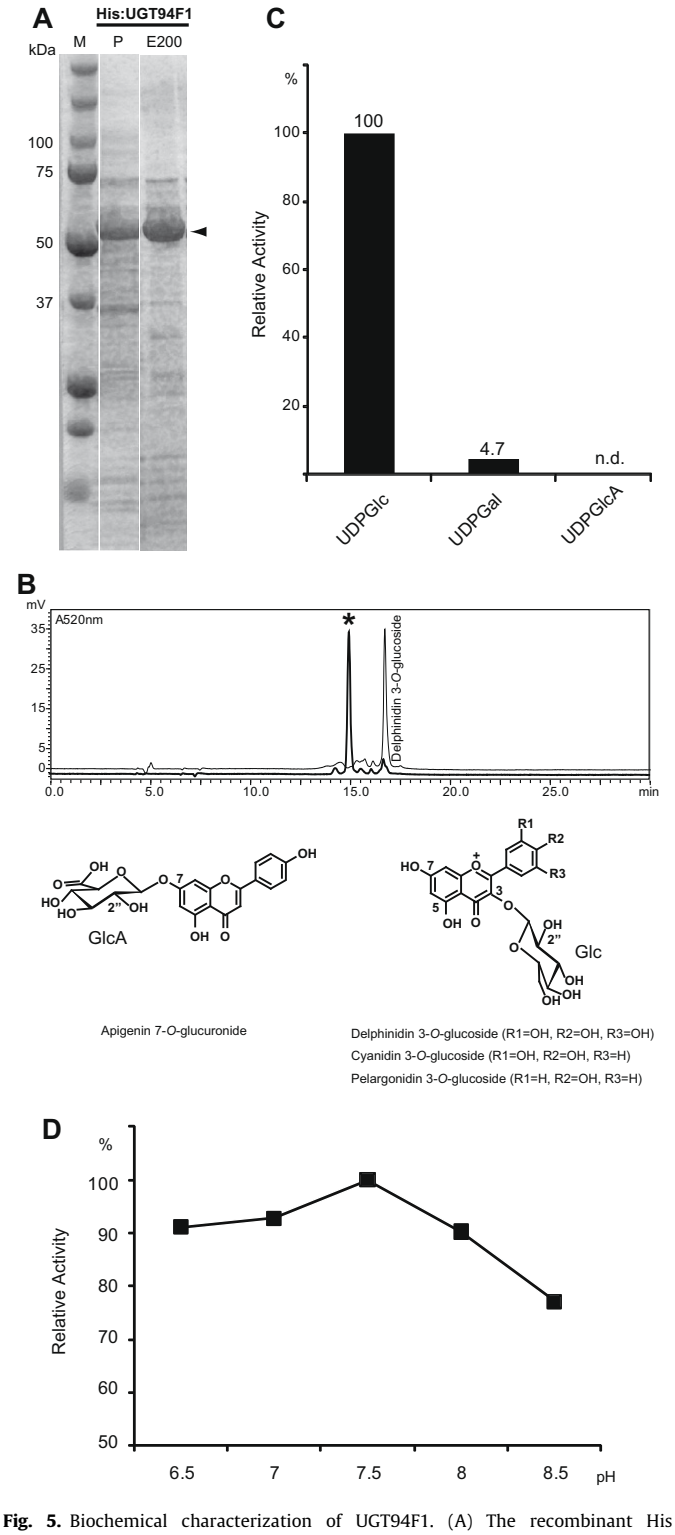

Fig. 5. Biochemical characterization of UGT94F1. (A) The recombinant His (x6)::UGT94F1 fusion protein (arrowhead) was expressed in *E. coli*, purified by a His Trap™ HP column, and detected using Coomassie Brilliant Blue (CBB) staining. M: molecular size marker, P: pellet fraction, E200: eluted fraction with 200 mM imidazole. (B) Chromatograms at abs 520 nm of reaction mixtures of UDP–Glc and delphinidin 3-*O*-glucoside in the absence (thin line) or presence (thick line) of the enzyme. The asterisk indicates a new product given by UGT94F1. (C) Relative sugar donor specificity of UGT94F1. Delphinidin 3-*O*-glucoside was used as the sugar acceptor. The highest specific activity on UDP–glucose is set as 100%. n.d. indicates "not detected". (D) Optimal pH of UGT94F1 for delphinidin 3-*O*-glucoside was tested in a range from pH 6.5 to 8.5 using potassium phosphate buffer (KPB). The highest activity was taken to be 100%.

cose are 0.32 ± 0.05 and 0.59 ± 0.11 mM, respectively. The sugar donor of UGT94F1 was preferably UDP–glucose (Fig. 5C), and the optimal pH of this enzyme was estimated to be 7.5 for the catalysis on delphinidin 3-*O*-glucoside in a range between pH 6.5 and 8.5 (Fig. 5D). Taken together, we conclude that UGT94F1 is a *V. persica* anthocyanidin 3-*O*-glucoside-2″-*O*-glucosyltransferase (A3G2″GlcT).

2.8. Expression analyses of UGT88D8 and UGT94F1 genes

To probe the organ distribution of *UGT88D8* and *UGT94F1* transcripts, RT-quantitative PCR (RT-qPCR) analysis was performed on separate organs from *Veronica* plants (Fig. 6). The *UGT88D8* gene was significantly expressed in petals, which is clearly in accordance with the preferred accumulation of the 7-*O*-glucuronosyl apigenin in this tissue. These data, together with the consistency of apigenin being accepted by recombinant UGT88D8 as the best substrate among tested (Fig. 3d), and being the core structure of glucuronides that are accumulated as major flavones in the petals of *V. persica*, suggest that UGT88D8 plays key role in blue flower coloration of *V. persica* by participating in the formation of co-pigment **2**. On the other hand, while moderate expression of *UGT88D8*, and comparable level of F7GAT activity was detected from the crude extracts of the leaves (Supplementary Fig. 1), a very low level, if any, of **2** was identified in the leaves by LC–MS analysis. Therefore, in the case of the leaf, the aglycone substrate for UGT88D8 is not likely to be easily available as compared to the petal. Alternatively, UGT88D8 might catalyze 7-*O*-glucuronosylation of other flavonoids in the leaf.

For *UGT94F1*, substantial level of expression in the petals was observed, supporting the idea that UGT94F1 is involved in the formation of anthocyanin pigment **1** by catalyzing glucosylation of sugar moiety of delphinidin 3-*O*-glucoside at the 2-hydroxy group (Fig. 6). The expression of *UGT94F1* in other organs such as stem and leaf suggest that UGT94F1 might play some biological role by accepting unknown substrates.

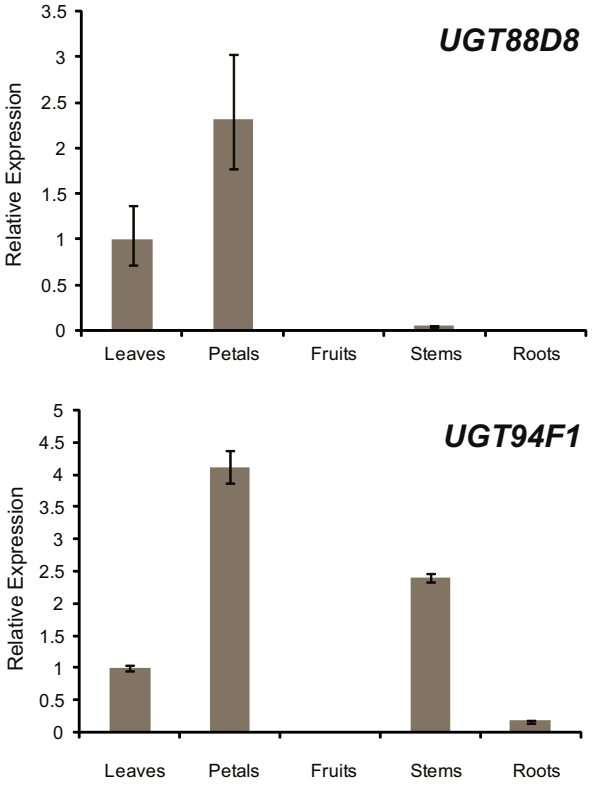

Fig. 6. Organ-specific distribution of *UGT88D8* and *UGT94F1* transcripts. Expression analysis of the *UGT88D8* gene was performed by RT-qPCR. These graphs show the relative expression of *UGT88D8* (AB465708) and *UGT94F1* (AB514127) in comparison with the reference gene, *V. persica rRNA* (AF509785).

3. Concluding remarks

In conclusion, we analyzed flavonoids of blue petals of *V. persica* and found the anthocyanin **1** and the flavone **2** as two main flavonoids. We then show the evidence of the bathochromic effects of **2** on coloration toward **1**, strongly suggesting that an intermolecular co-pigmentation between these two flavonoids occurs in *planta*. In addition, the relatively higher pH of the petals and extensive aromatic acylated delphinidin-type anthocyanins should contribute to the blue coloration.

By reverse genetics, we identified *V. persica* flavonoid 7-*O*-glucuronosyltransferase (UGT88D8) and anthocyanidin 3-*O*-glucoside-2″-*O*-glucosyltransferase (UGT94F1) as new members of functional clusters IIIb and IV of flavonoid UGTs, respectively. The identification of UGT88D8 confirmed that the F7GAT gene is widespread in Lamiales plants. UGT88D8 participate in flavone co-pigment **2** formation by providing a further glucuronosylation site for unidentified second GAT. On the other hand, UGT94F1 participates in the anthocyanin pigment **1** formation by providing further acylation site. Considering the preferred expression of the *UGT88D8* and *UGT94F1* genes in the petals as well as the bathochromic effects of **2** on **1**, both UGTs are involved in the bluish coloration of *V. persic*a flowers. Our findings herein not only establish the major components of a naturally occurring blue flower and their biosynthetic enzyme genes, but also provide promising tools for the molecular breeding of flowers with novel colors via the modification of pigments and co-pigments.

4. Experimental

4.1. Plant material

V. persica plants grown at Toyo University (Gunma, Japana) was used in this work. 530 g (fresh weight) of petals were collected on spring.

4.2. Chemical

Delphinidin chloride, apigenin, luteolin, diosmetin, chrysoeriol, kaempferol, quercetin, and naringenin were purchased from Funakoshi (Tokyo, Japan). Scutellarin was prepared as previously described (Noguchi et al., 2009). Baicalein, UDP–galactose, UDP–glucose, and UDP–glucuronic acid were purchased from Sigma (Germany).

4.3. MS measurement

High-resolution TOF-MS analysis of **1** and **2** was performed using a Q-TOF Premier mass spectrometer (MICROMASS, Manchester, UK) fitted with a Z-spray electrospray ion source (ESI) operated in a positive V mode at a 3-kV capillary voltage, and a 35.0-kV cone voltage. In the reference channel of the Lockspray ion source, to provide a lock mass ion at m/z 556.2771 $[M+H]^+$, a 0.6 ng/mL solution of leucine enkephalin in 50% MeCN and 0.1% (v/v) HCO_2H was continually delivered using a Jasco PV-2085 Plus semi-micro-HPLC pump system at a flow rate of 0.01 ml/min.

LC-TOF-MS analysis of the petal extract was carried out using the mass spectrometer in the positive V mode under the conditions described above. A Shodex-Asahipack ODP-40-3E

column (2.0 mm × 150 mm, Showa Denko, K. K. Japan) was used for LC on a LC-20AD HPLC (Shimadzu Co., Kyoto, Japan) with a ternary solvent system comprised of H_2O containing 0.1% (v/v) HCO_2H (A), CH_3CN containing 0.1% (v/v) HCO_2H (B). Each sample was eluted using a linear gradient of 10–60% of solvent B in solvent A for 20 min at a flow rate of 0.2 ml/min followed by 60% of solvent B for 5 min.

LC-TOF-MS analysis of the enzyme reaction mixtures was carried out. Develosil C30-UG-3 column (2.0 mm × 150 mm, Nomura Chemical, Aichi, Japan) was used for LC on a LC-20AD HPLC (Shimadzu Co., Kyoto, Japan) with a ternary solvent system comprised of H_2O containing 0.1% (v/v) HCO_2H (A), CH_3CN containing 0.1% (v/v) HCO_2H (B). Each sample was eluted using a linear gradient of 50–90% of solvent B in solvent A for 20 min at a flow rate of 0.2 ml/min and then with 90% of solvent B for 5 min. The column eluent was applied to the Q-TOF Premier in the negative V mode at a 3-kV capillary voltage and a 35.0-kV cone voltage. The reference, leucine enkephalin indicates m/z 554.2615 $[M-H]^-$.

4.4. NMR measurement

The ^1H NMR, ^{13}C NMR, $^1H\{^{13}C\}$-HSQC, $^1H\{^{13}C\}$-HMBC, TOCSY, DQF-COSY and ROESY spectra of **1** and **2** were obtained on a AVANCE-750 spectrometer (BRUKER BIOSPIN, Germany). The observation frequency for ^1H and ^{13}C measurement was 750.13 MHz and 188.62 MHz, respectively. Compound **1** was dissolved in a 10% (v/v) TFA–d/CD_3OD mixture. Compound **2** was dissolved in CD_3OD. The residual proton peaks and ^{13}C peaks of CD_3OD were used as the internal standard (δ 3.30 for ^1H and δ 48.97 for ^{13}C).

4.5. pH measurement and co-pigment assay

Fresh *V. persica* petals (2 g) was frozen at −80 °C and homogenized. The pH of the supernatant of the pressed juice was measured with an F-22 pH meter with a 6069-10C electrode (HORIBA Ltd., Japan).

4.6. HCl hydrolysis of 1 and HPLC analysis of anthocyanidin

Compound **1** (0.1 mg) was dissolved in 6 N HCl (0.2 ml) and kept at 100 °C for 20 min. The hydrolyzed anthocyanidin was extracted with 1-pentanol (0.2 ml).

HPLC conditions: an ODS-A312 (6 mm × 150 mm, YMC Co. Ltd., Japan) column, a solvent flow rate of 1 ml/min, and detection at an absorbance of 600–400 nm on a photodiode array detector SPD-M10A (Shimadzu Co. Ltd.). Under these HPLC conditions, the retention time and λ_{max} of delphinidin were 4.0 min and 534 nm, respectively, which was identified in comparison with authentic delphinidin chloride.

4.7. Pigment extraction

Petals of *V. persica* (530 g fresh weight) were lyophilized, pulverized, and extracted with H_2O–MeOH (2 L, 3:7, v/v) of containing 0.1% (v/v) TFA under room temperature overnight. After filtration, the extract was evaporated up to a quarter of its volume under vacuum. The solution was applied to HP-20 (200 ml) (Mitsubishi Chemical Co. Ltd., Japan) and afterwards washed with H_2O; the flavonoid fraction was eluted with H_2O–CH_3CN (800 mL, 4:1, v/v) and H_2O–CH_3CN (400 mL, 1:1, v/v) containing 0.1% (v/v) TFA. The H_2O–MeCN (4:1, v/v) eluate was concentrated and, after being washed with H_2O, was applied to a Sephadex LH-20 (Amarshem Pharmacia Biotech, UK). The column was eluted with H_2O–CH_3CN (9:1, v/v, 1.3 L) containing (v/v) 0.1% TFA, H_2O–CH_3CN (600 mL, 4:1, v/v) containing (v/v) 0.1% TFA, H_2O–CH_3CN (400 mL, 3:7, v/v) containing (v/v) 0.1% TFA, H_2O–CH_3CN (400 mL, 1:1, v/v) containing (v/v) 0.1% TFA, and H_2O–acetone (1:1, v/v) in a stepwise manner. The MeCN–H_2O (1:9) fraction, which contained anthocyanins, was further purified by prep HPLC. The HPLC was accomplished with the use of ODS (Capcell Pak C-18-UG-80, 2 cm × 25 cm, Shiseido Ltd., Japan) with a flow rate of 6 ml/min and monitoring at A270 nm. The solvent systems used included a linear gradient elution for 60 min using 20–46% of solvent B (CH_3CN–H_2O (1:1) containing 0.1% (v/v) TFA) in solvent A (H_2O containing 0.1% (v/v) TFA), 10 min using 20% of an isocratic elution, and further elution for 15 min with 46% of solvent B isocratically. This chromatogram gave six fractions. The main pigment Fr.3 containing **1** was further purified by prep HPLC. The HPLC was accomplished with the use of YMC-PAK ODS-A (2 cm × 25 cm, YMC Co. Ltd., Japan) with a flow rate of 6 ml/min and monitoring at A270 nm. The solvent systems used included a linear gradient elution for 40 min using 0–100% of solvent B (50 mM KH_2PO_4 in MeOH:H_2O (1:4, v/v) containing 0.1% (v/v) TFA) in solvent A (50 mM KH_2PO_4 containing 0.1% TFA). Anthocyanin **1** (2.3 mg) was obtained in this way.

The H_2O–acetone (1:1, v/v) fraction which contained co-pigment **2** was further purified by prep HPLC. The HPLC was accomplished with the use of ODS (Capcell Pak C-18-UG-80, 2 cm × 25 cm, Shiseido Ltd., Japan) as described above. Co-pigment **2** was obtained in 14 mg by repeating this chromatogram.

4.8. Co-pigment analysis and absorption spectra of petals

The co-pigment effects of **2** with **1** were examined as follows. First, compound **1** and **2** were dissolved to 100 mM in dimethyl sulfoxide (DMSO). Then, compound **1** in DMSO was diluted to 1 mM in a McIlvaine buffer (pH 6.2), and 1–6 mM of **2** in DMSO was added to the solution. The addition of six equivalents of **2**–**1** is an upper limit for a clear solution in this condition. The McIlvaine buffer was made by mixing 0.1 M of citric acid and 0.2 M of a Na_2HPO_4 solution to adjust to pH 6.2. Ten minutes after mixing, their visible absorption spectra at 780–380 nm and the colorimetric values of a C.I.E. $L^*a^*b^*$ were measured (C.I.E., http://www.cie.co.at/index_ie.html). The absorption spectra for the observation of co-pigment effects were measured on a Shimadzu UV-2500PC (Shimadzu Co. Ltd., Japan) with a 10 mm crystal cell. The colorimetric values of a C.I.E. $L^*a^*b^*$ system under a C light source were measured with color meter CR-200 for petals and CT-210 for the solution (Minolta, Japan). The visible spectra of fresh veronica petals were measured using a UV-2500PC spectrophotometer (Shimadzu Co., Japan).

4.9. Molecular cloning

Total RNA was extracted from the petals of *V. persica* using an RNeasy Plant Mini Kit (QIAGEN, Germany). cDNAs were synthesized from 1 μg of total RNA using a First-strand Synthesis System for RT-PCR (Invitrogen, CA). To obtain partial cDNA of UGT88D8, PCR with rTaq DNA polymerase (TaKaRa Bio Japan) was run at 94 °C for 3 min followed by 30 cycles at 94 °C for 1 min, 54 °C for 1 min, and 72 °C for 2 min using the AmF7GAT-Fw1 (5′-GTGATAG ATTTCTTTTGCAAT-3′) and AmF7GAT-Rv3 (5′-ACCCTATTCATCCTCT GCTCC-3′) primers for amplification of the fragment of *UGT88D8* gene, and the AmUGT94C-Fw5 (5′-CTTGTGTACCACAGCCAT-3′) and AmUGT94C-Rv3 (5′-GCTTTCTGTGATAGAACTCCA-3′) primers for amplification of the fragment of the *UGT94F1* gene. Amplified fragments were subcloned into pCR-TOPO II (Invitrogen, CA). Sequencing reactions were conducted using a BigDye-Terminator ver.3.1 cycle sequencing kit (Applied Biosystems, CA) and then analyzed using a 3100 Genetic analyzer (Applied Biosystems, CA). Because *UGT88D8* and *UGT94F1* had an incomplete open reading frame, the 5′- and 3′-ends were amplified with a GeneRacer kit

(Invitrogen, CA) and the following primer sets: GR-VpUGT88D8-Rv (5′-TTCCAGGAGGGTTTCGAACGGACCATA-3′) and VpUGT88D8-nest-Rv (5′-CTAGAGGTGCAACGAATAAAACTT-3′) for 5′-RACE, GR-Vp UGT88D8-Fw (5′-TATGGTCCGTTCGAAACCCTCCTGGAA-3′) and Vp UGT88D8-nest-Fw (5′-AGGATCCTGACCTGGAAACA-3′) for 3-RACE, GR-VpUGT94F-Rv (5′-CAGAGTTCCAACCCTTTGGCCACTTCT-3′) and VpUGT94F-nest-Rv (5′-CTGGCTCATCTTTCTCATCAGAA-3′) for 5′-RACE, and GR-VpUGT94F-Fw (5′-CCGTGGGCAGCCAAACAC GCGTTATCTCA-3′) and VpUGT94F-nest-Fw (5′-ACTGGCTCGCTTCT TCCTTATGAT-3′) for 3′-RACE.

4.10. Heterologous expression

The coding sequence of UGT88D8 and UGT94F1 was amplified by PCR using the specific primers of NdeI-VpF7GAT-Fw (5′-CACC CATATGGAAGACACAATCATCCT-3′) and XhoI-VpF7GAT-Rv (5′-CTC GAGTTTTTACCCAATAACCAACTTGAT-3′) for UGT88D8, and primers of NdeI-VpUGT1-Fw (5′-CACCCATATGGAGAAAGAAGAAGCAAAAA TG-3′) and BamHI-VpUGT1-Rv (5′-GGATCCTCAATCACATTTCTGCAA CTT-3′) for UGT94F1. The amplified fragment was cloned into a pENTR-Directional-TOPO vector (Invitrogen, CA) and sequenced to confirm the absence of PCR errors. The plasmid of UGT88D8 and UGT94F1 cDNAs was digested using NdeI and XhoI, and NdeI and BamHI, respectively. The resulting DNA fragment was ligated with a pET-15b vector (Novagen) that had previously been digested with NdeI and XhoI, and NdeI and BamHI. The resultant plasmid was transformed into *E. coli* BL21 (DE3). The transformant cells were prepared as previously described in Noguchi et al. (2008). The recombinant *E. coli* cells were harvested by centrifugation (7000*g*, 15 min), washed with distilled H_2O, and resuspended in buffer A (20 mM sodium Pi (pH 7.4), containing 14 mM 2-mercaptoethanol and 0.5 M NaCl) containing 20 mM imidazole. The cells were disrupted at 4 °C by five cycles of ultrasonication (where one cycle corresponds to 10 kHz for 1 min followed by an interval of 1 min). The cell debris was removed by centrifugation (7000*g*, 15 min). To the supernatant solution, polyethyleneimine was slowly added to a final concentration of 0.12% (v/v). The mixture was allowed to stand at 4 °C for 30 min, followed by centrifugation (7000*g*, 15 min). The supernatant was applied to a HisTrap™ HP column (1 ml, GE Healthcare Bio-Science) that had been equilibrated with buffer A containing 20 mM imidazole. The column was washed with buffer A containing 20 mM imidazole, and the enzyme was eluted with buffer A containing 200 and 500 mM imidazole. The active column-bound fractions were concentrated and desalted using VIVASPIN 30,000 MWCO (VIVASCIENCE, Hannover, Germany), followed by substitution with buffer B (20 mM potassium Pi (pH 7.5), containing 14 mM 2-mercaptoethanol). The protein concentration was determined using the Bradford method (Bradford, 1976) with bovine serum albumin as a standard. SDS–PAGE was carried out according to the method of Laemmli (Laemmli, 1970), and the proteins in the gels were visualized by Coomassie Brilliant Blue R250.

4.11. Enzyme assays and kinetics

The standard reaction mixture (50 μl) consisted of a 100 mM glycosyl acceptor, a 2 mM glycosyl donor, a 50 mM potassium phosphate buffer (pH 7.5), and enzymes. After a 10-min pre-incubation of the mixture without the enzyme at 30 °C, the reaction was initiated by addition of enzyme. After incubation at 30 °C for 30 min, the reaction was stopped by the addition of 50 μl of CH_3CN containing 0.5% (v/v) TFA. Reaction mixtures containing flavones/flavonols were analyzed using reversed-phase HPLC on the column Develosil C30-UG-5 (4.6 mm i.d. × 150 mm, Nomura Chemical, Aichi, Japan) with a linear gradient of 18 to H_2O–CH_3CN (37:63, v/v) containing 0.1% (v/v) TFA for 10 min and further elution for 5 min with 63% at a flow rate of 0.6 ml/min. Reaction mixtures containing anthocyanins were analyzed using reversed-phase HPLC on the column Shodex RSPak DE-413L (4.6 mm i.d. × 250 mm, SHOWA DENKO, Kanagawa, Japan) with a linear gradient of H_2O–CH_3CN (1:9 to 1:1, v/v) containing 0.5% (v/v) TFA for 15 min and then held at this composition for 10 min at a flow rate of 0.6 ml/min. Flavones/flavonols was detected at A280 nm, and anthocyanins at A520 nm using LC-2010HT HPLC system with a SPD-M20A photodiode array detector (Shimadzu, Kyoto, Japan).

Crude enzyme fractions were prepared from each sample (80 mg) of *V. persica* petals and leaves 80 mg (fresh weight) using a P-PER Plant Protein Extraction kit (Thermo Scientific, IL, USA) according to standard procedures for using the standard assay system (see above) in the presence or absence of UDP–GlcA (Supplementary Fig. 1). To determine the initial velocity of recombinant UGT88D8, the assays were carried out under steady-state conditions using the standard assay system with various substrate concentrations. The apparent *km* and *k*cat values for the glucuronosyl donor and acceptor substrate in the presence of a saturating concentration of the counter substrate were determined by fitting the initial velocity data to the Michaelis–Menten equation using non-linear regression analysis (Segel, 1975; Leatherbarrow, 1990).

4.12. RT-qPCR

Total RNA was extracted from each *V. persica* organ using the RNeasy Plant Mini Kit (QIAGEN, CA). cDNAs were reverse-transcribed from 1 μg of each total RNA with SuperScript III (Invitrogen, CA). RT-qPCR was performed using a TaqMan probe in a 7500 Real-Time PCR System (Applied Biosystems, CA) as described in Lanot et al. (2006). Gene-specific primer sets for *UGT88D8* (qVpF7GAT-Fw: 5′-GCGGTTTCGGCCTCTGT-3′ and qVpF7GAT-Rv: 5′-TCCGATATCTTGAGGGATGATTTC-3′), for *UGT94F1* (qVpUGT1-Fw: 5′-CCGTGGGCAGCCAAAC-3′ and qVpUGT1-Rv: 5′-GCACCTG ATGCCATAAACCA-3′), and for *rRNA* (Accession AF509785) (VprRNAq-Fw: 5′-GCGGAAGGATCATTGTCGAT-3′ and VprRNA-qRv: 5′-CTAGCGGGCGGAGCTTATTA-3′) were designed using Primer Express 3.0 software (Applied Biosystems, CA). The results were normalized to the reference gene rRNA and always expressed as expression ratios relative to a 'control' value using the ΔΔCt method (Applied Biosystems, CA). The standard deviations correspond to half the range of the expression between $2^{-(\Delta\Delta Ct+s)}$ and $2^{-(\Delta\Delta Ct-s)}$, where s is the SD of ΔΔCt ($n = 2$).

Acknowledgements

We thank Professor P.I. Mackenzie (Flinders University, Australia) for assigning UGT numbers, Dr. A. Noguchi (University of Tokyo) for the productive discussions related to this study, and Dr. J. Murata (SUNBOR) for critical reading of the manuscript. We also thank Dr. Y. Katsumoto, Mrs. K. Iwasa, Mrs. A. Saito, Ms. N. Nakamura, Ms. H. Toyonaga (Suntory), and Dr. M. Horikawa (SUNBOR) for their excellent technical support with the experimental procedures.

Appendix A. Supplementary data

Supplementary data associated with this article can be found, in the online version, at doi:10.1016/j.phytochem.2010.02.008.

References

Aida, R., Yoshida, K., Kondo, T., Kishimoto, S., Shibata, M., 2000. Copigmentation gives bluer flowers on transgenic torenia plants with the antisense dihydroflavonol-4-reductase gene. Plant Sci. 160, 49–56.

Asen, S., Norris, K.H., Stewart, R.N., 1972. Copigmentation of aurone and flavones from petals of *Antirrhinum majus*. Phytochemistry 11, 2739–2741.

Boulton, R., 2001. The copigmentation of anthocyanins and its role in the color of red wine. Am. J. Enol. Vitic. 52, 67–87.
Bradford, M.M., 1976. A rapid and sensitive method for the quantitation of microgram quantities of protein utilizing the principle of protein–dye binding. Anal. Biochem. 72, 248–254.
Frydman, A. et al., 2004. Citrus fruit bitter flavors: isolation and functional characterization of the gene Cm1, 2RhaT encoding a 1, 2 rhamnosyltransferase, a key enzyme in the biosynthesis of the bitter flavonoids of citrus. Plant J. 40, 88–100.
Fukada-Tanaka, S., Inagaki, Y., Yamaguchi, T., Saito, N., Iida, S., 2000. Colour-enhancing protein in blue petals. Nature 407, 581.
Fukui, Y., Tanaka, Y., Kusumi, T., Iwashita, T., Nomoto, K., 2003. A rationale for the shift in colour toward blue in transgenic carnation flowers expressing the flavonoid 3', 5'-hydroxylase gene. Phytochemistry 63, 15–23.
Goto, T., Kondo, T., 1991. Structure and molecular stacking of anthocyanins – flower color variation. Angew. Chem. Int. Ed. Engl. 30, 17–33.
Harborne, J.B., 1963. Plant polyphenols. X. Flavone and aurone glycosides of *Antirrhinum*. Phytochemistry 2, 327–334.
Harborne, J.B., Baxter, H., 1999. The Handbook of Natural Flavonoids, vol. 2. John Wiley and Sons, New York, USA.
Hirotani, M., Nagashima, S., Yoshikawa, T., 1998. Baicalin and baicalein productions of cultured *Scutellaria baicalensis* cells. Nat. Med. 52, 440–443.
Hirotani, M., Kuroda, R., Suzuki, H., Yoshikawa, T., 2000. Cloning and expression of UDP–glucose: flavonoid 7-*O*-glucosyltransferase from hairy root cultures of *Scutellaria baicalensis*. Planta 210, 1006–1013.
Katsumoto, Y. et al., 2007. Engineering of the rose flavonoid biosynthetic pathway successfully generated blue-hued flowers accumulating delphinidin. Plant Cell Physiol. 48, 1589–1600.
Kondo, T., Yoshida, K., Nakagawa, A., Kawai, T., Tamura, H., Goto, T., 1992. Structural basis of blue-color development in flower petals from *Commelina communis*. Nature 358, 515–518.
Kondo, T., Oyama, K.-I., Yoshida, K., 2001. Chiral molecular recognition on formation of a metalloanthocyanin: a supramolecular metal complex pigment from blue flowers of *Salvia patens*. Angew. Chem. Int. Ed. Engl. 40, 894–897.
Laemmli, U.K., 1970. Cleavage of structural proteins during the assembly of the head of bacteriophage T4. Nature 227, 680–685.
Lanot, A., Hodge, D., Jackson, R.G., George, G.L., Elias, L., Lim, E.K., Vaistij, F.E., Bowles, D.J., 2006. The glucosyltransferase UGT72E2 is responsible for monolignol 4-*O*-glucoside production in *Arabidopsis thaliana*. Plant J. 48, 286–295.
Leatherbarrow, R.J., 1990. Using linear and non-linear regression to fit biochemical data. Trends Biochem. Sci. 15, 455–458.
Mackenzie, P.I. et al., 1997. The UDP glycosyltransferase gene superfamily: recommended nomenclature update based on evolutionary divergence. Pharmacogenetics 7, 255–269.
Masada, S., Terasaka, K., Oguchi, Y., Okazaki, S., Mizushima, T., Mizukami, H., 2009. Functional and structural characterization of a flavonoid glucoside 1, 6-glucosyltransferase from *Catharanthus roseus*. Plant Cell Physiol. 50, 1401–1415.
Mori, M., Kondo, T., Yoshida, K., 2008. Cyanosalvianin, a supramolecular blue metalloanthocyanin, from petals of *Salvia uliginosa*. Phytochemistry 69, 3151–3158.
Mori, M., Kondo, T., Yoshida, K., 2009. Anothocynian components and mechanism for color development in blue *Veronica* flowers. Biosci. Biotechnol. Biochem. 73, 2329–2331.
Morita, Y. et al., 2005. Japanese morning glory dusky mutants displaying reddish-brown or purplish-gray flowers are deficient in a novel glycosylation enzyme for anthocyanin biosynthesis, UDP–glucose: anthocyanidin 3-*O*-glucoside-2″-*O*-glucosyltransferase, due to 4-bp insertions in the gene. Plant J. 42, 353–363.
Noguchi, A., Fukui, Y., Iuchi-Okada, A., Kakutani, S., Satake, H., Iwashita, T., Nakao, M., Umezawa, T., Ono, E., 2008. Sequential glucosylation of a furofuran lignan, (+)-sesaminol by *Sesamum indicum* UGT71A9 and UGT94D1 glucosyltransferases. Plant J. 54, 415–427.
Noguchi, A., Fukui, Y., Horikawa, M., Fukuchi-Mizutani, M., Iuchi-Okada, A., Ishiguro, M., Kiso, Y., Nakayama, T., Ono, E., 2009. Local differentiation of sugar donor specificity of flavonoid 7-*O*-glycosyltransferase in Lamiales. Plant Cell 21, 1556–1572.
Okigawa, M., Hatanaka, H., Kawano, N., Matsunaga, I., Tamura, Z., 1971. Studies on the components of *Clerodendron trichotomum* Thunb. III. A new glycoside, a cacetin-7-glucurono-(1 → 2)-glucuronide from the leaves. Chem. Pharm. Bull. 19, 148–152.
Ono, E. et al., 2006. Yellow flowers generated by expression of the aurone biosynthetic pathway. Proc. Natl. Acad. Sci. USA 103, 11075–11080.
Osmani, S., Bak, S., Imberty, A., Olsen, C.E., Møller, B.L., 2008. Catalytic key amino acids and UDP–sugar donor specificity of a plant glucuronosyltransferase, UGT94B1. Plant Physiol. 148, 1295–1308.
Sawada, S., Suzuki, H., Ichimaida, F., Yamaguchi, M.A., Iwashita, T., Fukui, Y., Hemmi, H., Nishino, T., Nakayama, T., 2005. UDP–glucuronic acid:anthocyanin glucuronosyltransferase from red daisy (*Bellis perennis*) flowers. Enzymology and phylogenetics of a novel glucuronosyltransferase involved in flower pigment biosynthesis. J. Biol. Chem. 280, 899–906.
Segel, I.H., 1975. Enzyme Kinetics. Behavior and Analysis of Rapid Equilibrium and Steady-state Enzyme Systems. John Wiley and Sons, New York.
Shiono, M., Matsugaki, N., Takeda, K., 2005. Structure of the blue cornflower pigment. Nature 436, 791.
Tamura, K., Dudley, J., Nei, M., Kumar, S., 2007. MEGA4: molecular evolutionary genetics analysis (MEGA) software version 4.0. Mol. Biol. Evol. 24, 1596–1599.
Terahara, N., Callebaut, A., Ohba, R., Nagata, T., Ohnishi-Kameyama, M., Suzuki, M., 1996. Triacylated anthocyanins from *Ajuga reptans* flowers and cell cultures. Phytochemistry 42, 199–203.
Thompson, W.R., Meinwald, J., 1972. Flavonols: pigments responsible for ultraviolet absorption in nectar guide of flower. Science 177, 528–530.
Thompson, J.D., Higgins, D.G., Gibson, T.J., 1994. CLUSTAL W: improving the sensitivity of progressive multiple sequence alignment through sequence weighting, position-specific gap penalties and weight matrix choice. Nucl. Acids Res. 22, 4673–4680.
Verweij, W., Spelt, C., Di Sansebastiano, G.P., Vermeer, J., Reale, L., Ferranti, F., Koes, R., Quattrocchio, F., 2008. An H+ P-ATPase on the tonoplast determines vacuolar pH and flower colour. Nat. Cell Biol. 10, 1456–1462.
Vogt, T., Jones, P., 2000. Glycosyltransferases in plant natural product synthesis: characterization of a supergene family. Trends Plant Sci. 5, 380–386.
Yabuya, T., Nakamura, M., Iwashita, T., Yamaguchi, M., Takehara, T., 1997. Anthocyanin-flavone copigmentation in bluish purple flowers of Japanese garden iris (*Iris ensata* Thunb.). Euphytica 98, 163–167.
Yamazaki, M., Nakajima, J., Yamanashi, M., Sugiyama, M., Makita, Y., Springob, K., Awazuhara, M., Saito, K., 2003. Metabolomics and differential gene expression in anthocyanin chemo-varietal forms of *Perilla frutescens*. Phytochemistry 62, 987–995.
Yoshida, K., Kameda, K., Kondo, T., 1993. Diglucuronoflavones from purple leaves of *Perilla ocimoides*. Phytochemistry 33, 917–919.
Yoshida, K., Kitahara, S., Ito, D., Kondo, T., 2006. Ferric ions involved in the flower color development of the Himalayan blue poppy, *Meconopsis grandis*. Phytochemistry 67, 992–998.
Yoshida, K., Mori, M., Kondo, T., 2009. Blue flower color development by anthocyanins: from chemical structure to cell physiology. Nat. Prod. Rep. 26, 884–915.